Engineering Failure Analysis 97 (2019) 300–310

Contents lists available at ScienceDirect

Engineering Failure Analysis

journal homepage: www.elsevier.com/locate/engfailanal

Stress corrosion of an austenitic stainless steel expansion joint, a case study

M.J. Gomes da Silva[a,*], H.A.P. Fragoso[b], R.C.A.G. Barrio[a], J.L. Cardoso[a]

[a] Universidade Federal do Ceará, Department of Metallurgical and Materials, Brazil
[b] Universidade Federal do Rio Grande do Sul, Department of Metallurgical Engineering, Brazil

A B S T R A C T

The duct system is one of the structures that most need a series of conditions that require the system to have a certain flexibility of movement due to thermal stresses, changes in the direction of the duct system and the unevenness on the ground. Metal bellows are designed to provide flexibility to the system, however, to guarantee the proper properties in service one should consider the material used in the component manufacturing as well as the manufacturing process itself. This research aimed to study a case of failure due to the stress corrosion of an austenitic stainless steel expansion joint. For the assessment of the main factors that led to the failure of the expansion joint, some analyses were employed: microstructural characterization by optical microscopy and scanning electron microscopy (SEM); X-ray diffraction; solution annealing heat treatments and microhardness. The results showed that the cleaning conditions allowed pits and cavities to form on the inner surface of the bellows while the forming processes used in the bellows manufacturing of the expansion joints were responsible for providing the necessary metallurgical conditions for the nucleation and propagation of cracks from pits and cavities. From the results it was possible to enumerate a series of recommendations that take into account an adequate cleaning of the component as well as the appropriate thermal treatments to optimize the service life of the studied component.

1. Introduction

Expansion bellows joints basically consist of a flexible element that elastically absorbs the expansion or contraction of the piping system to which it is installed, giving flexibility to the system. Expansion bellows joints can also be applied in situations where space is reduced for possible change of direction in the piping system and also compensate for misalignments caused by mounting problems or due to irregular terrain [1,2].

The main movements that a joint can perform are the axial, lateral and angular movements. The axial movements involve both compression and elongation of the bellows parallel to its axis. The lateral movements occur when a lateral deflection is imposed by the displacement of one end of the bellows relative to another end in the direction perpendicular to its axis, so that the longitudinal axes of the welded ends remain parallel. The angular movement occurs when the bellows forms an arc of a circle, so that the ends of the joints tend to be perpendicular [1]. These movements are always relative between two section of a plant and they are caused by thermal expansion, pressure, internal forces, misalignment or foundation settlement [2].

An expansion bellow joint is an assembly designed to absorb contractions and expansion due to induced temperature, vibration, mechanical changes in the system and it is used in some structures to hold parts together like piping systems, ships, bridges, buildings and others. The expansion joint introduces a discontinuity in the tubing from a continuous medium to a discontinuous one [1,3].

Several problems can occur in the expansion bellows joints like warping, cracking, leaking fluids among others. These problems can cause stresses at connection points of some structures like pipes misaligning the installations [1].

One of the materials used in the manufacture of the expansion bellows joints is the AISI 304 austenitic stainless steel. This steel is

* Corresponding author.
E-mail address: mgsilva@ufc.br (M.J. Gomes da Silva).

https://doi.org/10.1016/j.engfailanal.2019.01.021
Received 19 June 2018; Received in revised form 28 November 2018; Accepted 2 January 2019
Available online 07 January 2019
1350-6307/

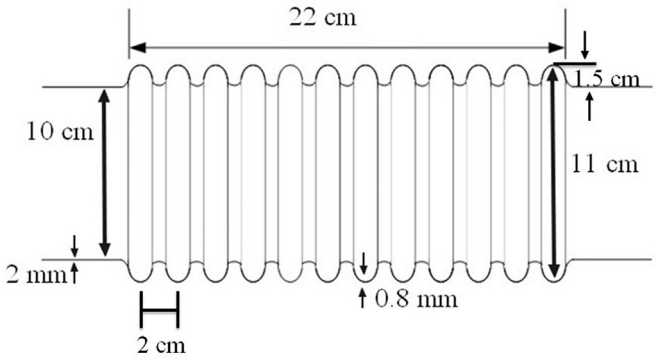

Fig. 1. Schematic drawing of the metal expansion bellows joints and the smooth tube with dimensions.

a Cr-Fe-Ni alloy which shows good corrosion resistance and is non-magnetic but may exhibit a certain amount of magnetism when subjected to cold work due to the formation of deformation-induced martensite. In addition to good corrosion resistance, AISI 304 exhibits good weldability and good formability, but under certain conditions, such as in environments containing chloride ions, the AISI 304 austenitic stainless steel is susceptible to localized corrosion [4–6]. This work aims to analyze the root cause of failure of a dismantled sample by visual examination by metallographic analysis using techniques like optical and Scanning Electron Microscopy (SEM), chemical analysis, X-ray diffraction and hardness tests.

2. Materials and experimental

2.1. Material

2.1.1. Samples dimensions

Five samples of a 304 austenitic steel were received as a cylindrical smooth tube, three new metal expansion bellows joints with weld ends and a metal expansion joint previously used in service. The dimensions of the expansion bellows joints and the smooth tube are shown in Fig. 1. In service, the plain tubes and the expansion bellows joints are joined by TIG welding. Inside the pipe/joint system is the passage of another pipe of 5.08 cm diameter. The inner region of the system is subjected to negative pressure to prevent the exchange of heat from the external environment to the duct that is located inside the pipe/joint system, thus, the system is required to maintain its integrity under environmental conditions, avoiding failures that cause the air to enter into the piping system and as a consequence the heat exchange from the medium to the interior of the system.

2.1.2. Chemical composition of the samples

The chemical compositions of smooth tube samples and metal expansion bellows joints were obtained by optical emission spectrometry technique on a SHIMADZU PDA-7000 Optical Emission Spectrometer as seen in Table 1.

2.1.3. Visual inspection of the received samples

All samples were inspected on their external and internal surfaces for signs of corrosion or other nonconformities. A flowchart (Fig. 2) shows all the steps of the analyses and measurements of this research.

2.2. Experimental methods and equipments

2.2.1. Microstructural characterization

For the microstructural characterization of the samples in the as received condition, a metallographic preparation was carried out. After the preparation of the samples, the micrographs were obtained from two techniques: Optical Microscopy and Scanning Electron Microscopy (SEM) Equipped with Electron BackScatter Diffraction (EBSD).

2.2.2. Metallographic preparation

Samples were obtained by cutting the smooth tube in the internal and external regions and the expansion bellows joints samples

Table 1
Chemical composition (wt%) of the samples studied in this work.

Samples	C	Si	Mn	Ni	Cr	Mo	Cu	Pb	Al	Nb
Smooth tube	0.051	0.62	1.50	8.23	17.9	0.20	0.098	0,013	0.016	0.15
Expansion bellows joints	0.042	0.051	1.31	8.26	18.73	0.14	0.041	0.041	0.012	0.093

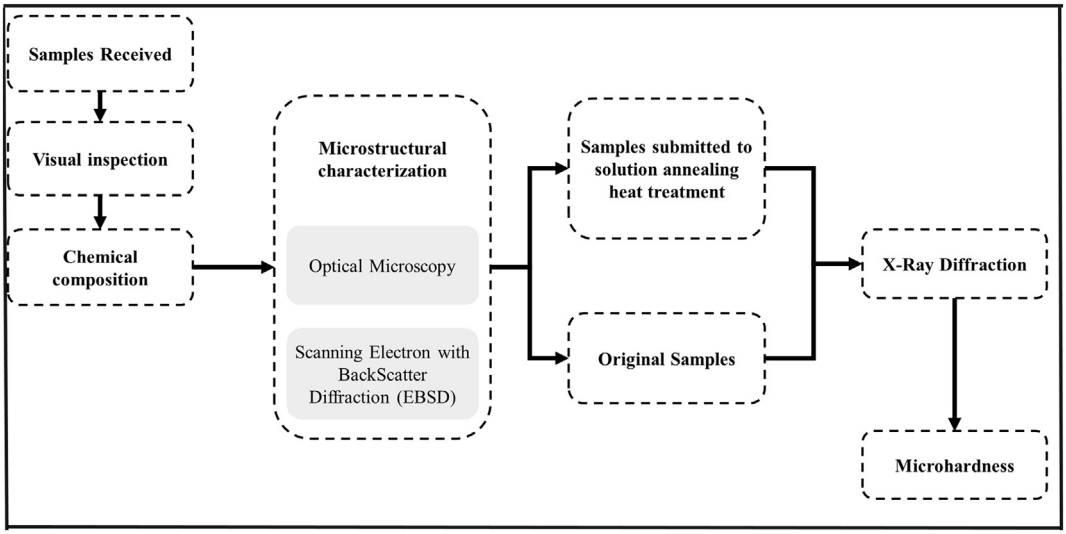

Fig. 2. Flowchart showing the steps of this research.

were obtained from the internal and external regions of the weld that cross the entire length of the joint and in the internal and external regions that are far from the weld. The position of the samples is shown in Fig. 3. The samples were embedded in synthetic resin (bakelite) and then sanded with silicon carbide paper with particle size of 180, 320, 400 and 600 mesh and then polished in diamond pastes with grain size of 6, 3 and 1 μm. After polishing, the samples were washed in running water, sprinkled with alcohol and hot-air-dried.

The microstructures were revealed by electrolytic etching where the arrangement of the cell consisted of a stainless steel plate as a cathode and the sample as the anode. To obtain a greater variety of structures, a series of electrolytes were used: first, a solution with 10% oxalic acid with a current density of 1 A/cm^2 and 1.5 min in length according to ASTM A 262 – 15 [7]; second, a 60% and 45% nitric acid with a voltage of 3 V and a duration of 1 to 3 s; and third, an Ammonium persulphate.

The etching time on some samples varied due to sample size and the applied current density. After etching, the samples were washed in running water and then with alcohol and then hot-air-dried.

2.2.3. Optical and scanning electron microscopy (SEM)

For the observations of the microstructures and other corrosion indicators, a ZEISS Optical Microscope and an Electronic Scanning Microscope PHILIPS XL-30 equipped Oxford Instruments HKL CHANNEL 5 Data Acquisition and Analysis Software for EBSD analysis were used.

2.2.4. Analysis in Electron Backscatter Diffraction (EBSD)

An EBSD analysis of a sample of the concertina region of a metal expansion joint was analyzed. The collected sample was embedded in synthetic resin and then sanded in 100, 200, 320, 400, 600 and 1200 mesh using a SiC sandpaper. After the sanding step, the sample was subjected to polishing in 6, 3 and 1 μm diamond paste and after manual polishing; it was subjected to automatic polishing on colloidal silica. The EBSD technique was used to confirm the presence of Body Cubic Center (BCC) martensite in the Faced Cubic Center (FCC) austenitic matrix.

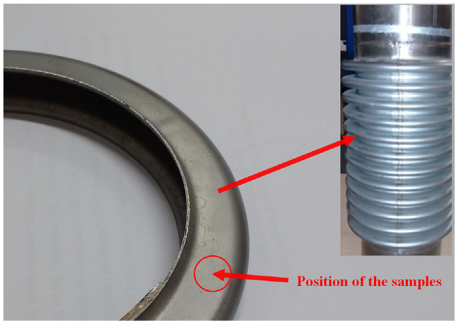

Fig. 3. Position of the samples on the metal bellow joint.

Table 2
Description of the labeled samples.

Samples	Description
A	External surface of the metal expansion bellows joints
B	Internal surface of metal expansion bellows joints
L	External surface of the smooth tube
L-Sol	Smooth tube solution annealed at 1050 °C for 30 min
B-Sol	Metal expansion bellows joints solution annealed at 1050 °C for 30 min

2.2.5. Solution annealing heat treatment

Solution annealing heat treatments were performed on a sample of the smooth tube and a sample of the accordion and cross section of a new metal expansion joint. The solution annealed treatment consisted in subjecting the samples to a temperature of 1050 °C over a period of 30 min. The samples were then cooled rapidly in water at room temperature.

2.2.6. X-ray diffraction

The x-ray diffraction spectra were obtained from samples of the flat tube, solution annealed flat tube and the bellows of expansion joint in a Philips® X'pert Pro diffractometer with step size of 0.013°, time per step of 100 s and 2 theta interval of 40°–120°. The source of radiation of CuKα (0.1540 nm) was used at 40 kV and 40 mA with monochromator.

2.2.7. Microhardness

A HMV Micro Hardness Tester SHIMADZU was used to perform the microhardness. For the tests, the samples were labeled and described in Table 2. In each sample, 6 measurements were performed in random regions using a load of 2.942 N (0.3 g) and the scale used was Vikers (HV).

3. Results and discussion

3.1. Chemical analyses

From the chemical composition, one can see that the carbon content of the expansion bellow joint and the smooth pipe are greater than 0.03% wt, so such steels subjected to temperatures ranging from 425 °C to 900 °C can form chromium carbides that reduce the corrosion resistance of these steels [8]. It is also observed, through the chemical analysis, that the samples do not have considerable levels of niobium or molybdenum. Molybdenum is an element that improves pitting corrosion and niobium is preferentially bound to carbon, concurring with chromium, reducing formation of chromium carbides in the sensitization temperature range [6,9]. Although the 304 steel posses no Mo, a residual composition of Mo was detected in the chemical composition analysis.

3.2. Visual inspection of samples received

Fig. 4 shows three samples as received: a smooth tube, a dismantled metal expansion joint and a new expansion joint, respectively. Fig. 5 shows the inner surface of the smooth tube. It is possible to note that the inner surface has a number of localized points of corrosion, suggesting that this region is suffering from pitting corrosion. Since the flat tube was not employed in service, the corrosion in the inner part suggests that the tube has undergone a corrosion process in a chloride environment in the storage or transport stage.

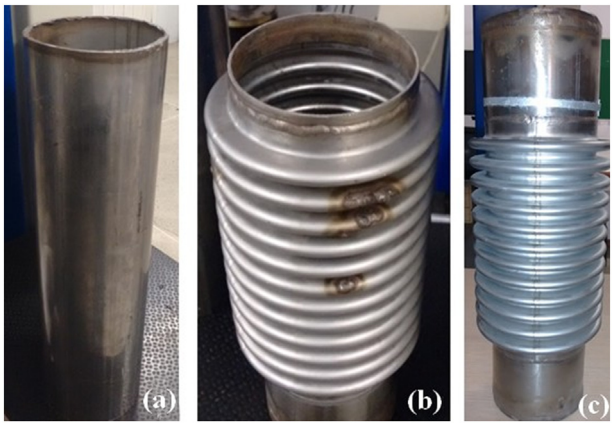

Fig. 4. Samples in the as received condition: (a) plain tube, (b) dismantled metal expansion joint, and (c) new metal expansion joint.

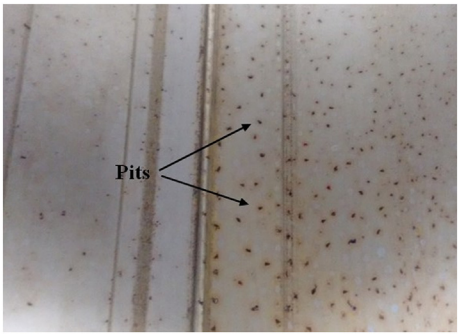

Fig. 5. Internal surface of the plain tube with some pits.

Fig. 6 shows the outer and inner region of a dismantled metal expansion joint after use. It is possible to observe signs of localized corrosion in the internal region, as well as in the internal and adjacent regions on the external surface of the expansion bellow joint. From Figs. 7 and 8 it is noted that the corrosions on the inner surface of the expansion bellows joints are located in specific regions, so that there are regions with more pronounced deterioration and regions that seem to have been little affected. The protrusions (oxides) in the corroded region indicate the presence of more intensified localized corrosion.

The visual inspection of the internal and external regions of the expansion bellows joints shows that only the internal region of the joints presented signs of corrosion, indicating that the internal surfaces of the joints may have been subjected to aggressive corrosive media such as machine wastes that can incorporate chloride ions. The external surface of the material showed no obvious signs of localized corrosion.

Fig. 8 shows a series of images of the samples collected from a new expansion joint in the outer and inner region of the longitudinal seam (TIG weld) of the bellows joint as well as in the inner and outer region opposite the weld. It is possible to note that in Fig. 8a and b on both the outer and inner surfaces of the TIG weld / metal interface there are signs of corrosion running parallel to the heat affected zone of the expansion joint, which is characteristic of the phenomenon of intergranular corrosion on these steels [6,8]. In the bottom side of TIG weld, in Fig. 8b, a greater deterioration is noticed, being a probable consequence of the differences in the galvanic properties of the weld seam - heat affected zone and base metal in transverse direction.

Fig. 8c shows an area opposite the weld region of the outer surface of a new metal expansion joint. In the outer region, there is no visible evidence of corrosion, but in Fig. 8d, which shows the internal surface of Fig. 8c, it is possible to observe that this region already shows a marked degree of generalized corrosion.

3.3. Microstructural characterization

The martensite slats can also be observed in the micrograph of the metal expansion joint obtained from the electrolytic etching using the HNO_3 nitric acid, as shown in Fig. 9a. The new expansion joint micrograph presents a series of small needles along its structure, whereas the micrograph of the smooth tube does not present them (Fig. 9b), but this does not mean that the smooth tube does not present a martensitic structure, but rather that the microstructure of the expansion joint presents a higher volume of martensite as a consequence of a greater conformation in the manufacturing process.

Fig. 6. Metal expansion joint already dismantled. (a) External region and (b) internal region of the joint. The sample was cut longitudinally for easy viewing.

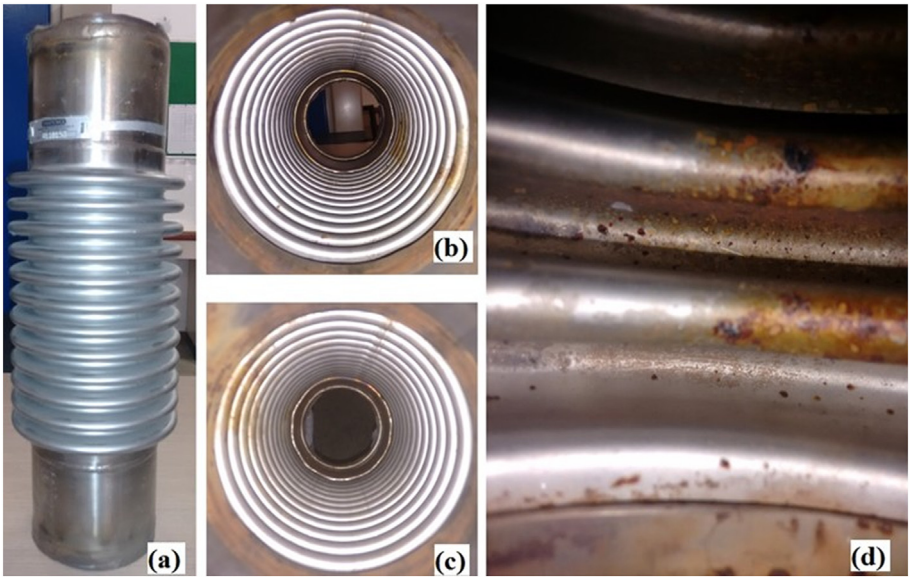

Fig. 7. New metal expansion joint: (a) profile, (b) inner region from top, (c) inner region from base, and (d) corroded internal surface.

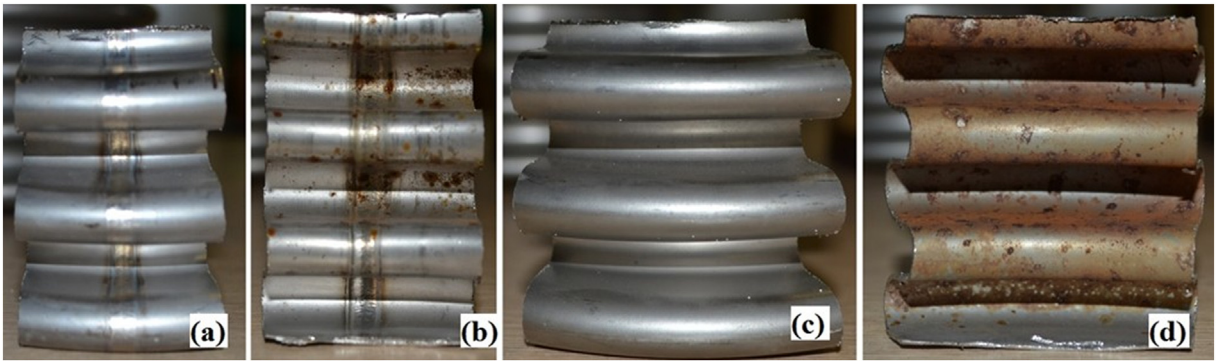

Fig. 8. Samples obtained from a new metal expansion joint. (a) External region of the weld, (b) internal region of the weld area, (c) external region of the area opposite the weld, and (d) internal region of the area opposite the weld.

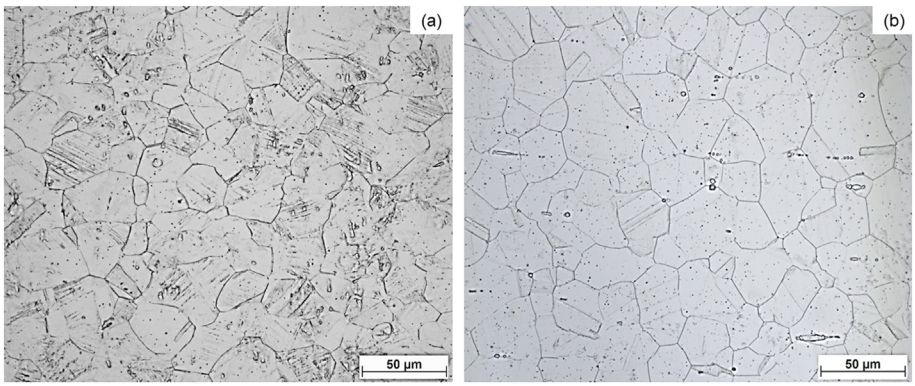

Fig. 9. Optical micrograph of the (a) new metal expansion joint and (b) smooth tube. Microstructures obtained from the electrolytic etching with (a) 60% nitric acid (b) and 40% nitric acid.

The morphologies of these needles resemble the morphology of martensite presented in the work of Milad et al. [10]. Austenitic stainless steels are not heat curable, but in cold work they can form deformation induced martensite, which corroborates the fact that the expansion bellows joints suffered a greater deformation when compared with the smooth tube [9–11].

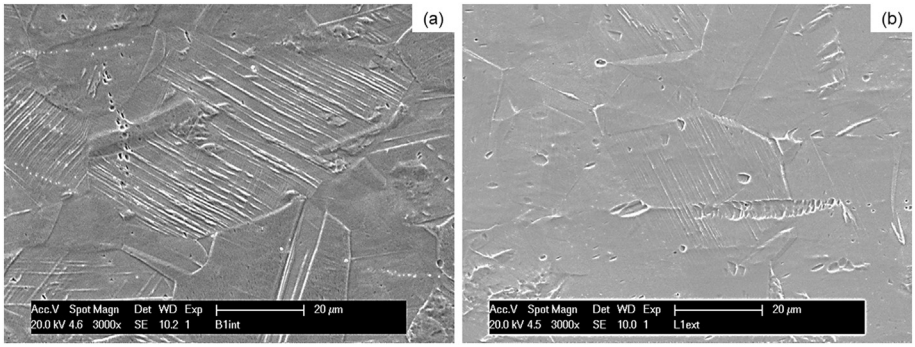

Fig. 10. SEM of the inner region of the (a) new metal expansion joint and (b) smooth tube.

Fig. 10 shows a comparison between the microstructures of the metal expansion joint (Fig. 10a) and the smooth tube (Fig. 10b) obtained by SEM. It is observed due to a more intense conformation process, the metal expansion joint presents a larger volume of martensite. Fig. 11 shows the martensite and also the grain boundaries of the austenite. It is noted that the grains do not have a homogeneous size, which is characteristic of a material that has undergone a metal forming process. To confirm the presence of the deformation induced martensite, an EBSD measurement on the metal expansion joint was performed. Fig. 12 shows the presence of the martensitic structure within the austenitic grain through EBSD.

According to Briant and Ritter [12] the strain-induced martensite in the AISI 304 austenitic stainless steel despite improving the mechanical strength of the steel, has a negative effect on the sensitization. They found that martensite is a site of carbide nucleation because of its BBC structure, so that chromium and carbon diffuse more rapidly than in the FCC structure of the austenite. Moreover, in martensite the solubility of carbon is lower than in austenite, further favoring the formation of chromium carbides [12,13].

Cold work at certain levels induces the formation of martensite and may contribute to the increase of toughness [14,15]. However, martensite platelets may also represent sites of stress concentration on the surface and as a consequence, the number of anodic sites on the surface of the material causing a reduction in localized corrosion resistance, such as a reduction in resistance to stress corrosion or pitting corrosion [5,9].

The austenitic matrix has a lower energy level than the deformation induced martensite, in addition, the cold working action increases the density of dislocations in certain regions, also causing at these points a change in the diffusion kinetics of the alloying elements which can promote a reduction in localized corrosion resistance by the appearance of anodic sites [16,17].

Fig. 13 shows the micrograph of the seam welding region of a dismantled metal expansion joint. Inside this metal expansion joint, there was a duct where liquid oxygen went through. The pressure in and out the metal expansion joint was the ambient pressure. It is possible to notice that this region displays a series of cracks that are indications of integranular corrosion in function of a possible formation of carbides in the contours of grain due to the welding process.

In the austenitic stainless steels the integranular corrosion is the result of the sensitization process that these steels suffer when they are submitted to thermal treatments in the temperature range of 425 °C to 900 °C, as in the welding processes [17,18]. The chromium carbides that form in the grain boundaries deplete the adjacent region of this element, rendering the region susceptible to corrosion. This type of corrosion is common on austenitic stainless steels with carbon contents greater than 0.03% (wt) or when they do not have elements with carbon affinity, such as niobium, vanadium and titanium [5,19].

Fig. 14 shows some discontinuities (cracks and cavities) found along the inner region of a new metal expansion joint. Cracks along the inner surface of the joints indicate that the material has a certain level of residual stress. It is also possible to notice that these cracks nucleate in regions that show signs of more advanced deterioration. The cracks originate in cavities that are consequences of the deterioration process that the material underwent. These cavities or pits are regions that concentrate tensions and because of this

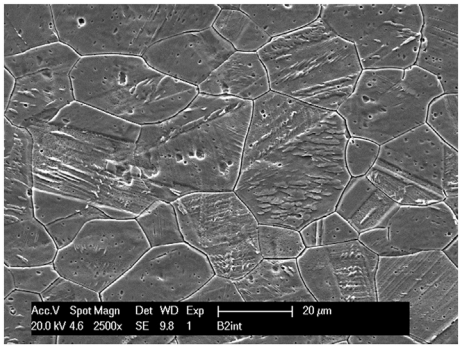

Fig. 11. SEM of the inner region of a new metal outlet.

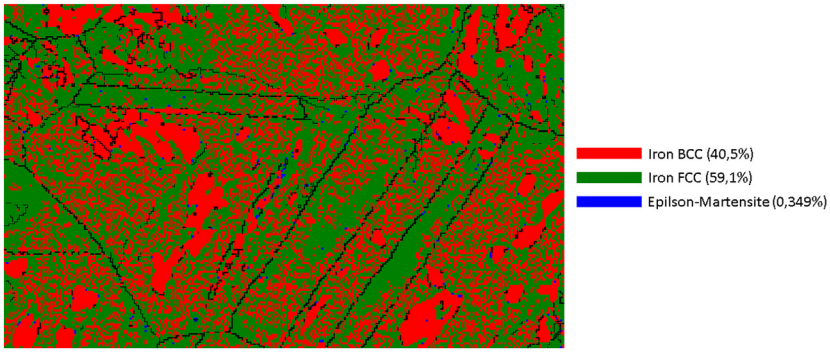

Fig. 12. EBSD of the inner region of the new metal expansion joint.

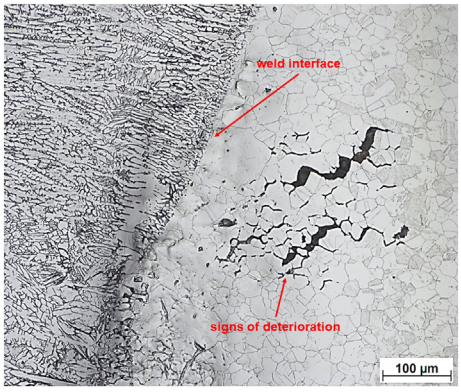

Fig. 13. Optical micrograph of the weld interface of a used metal expansion joint.

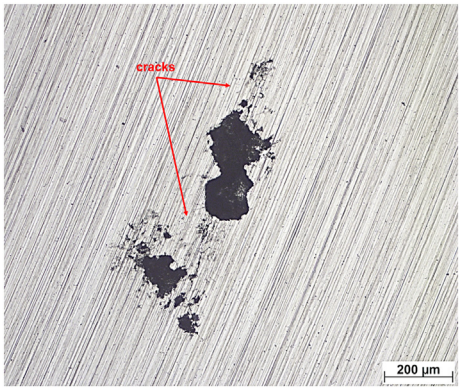

Fig. 14. Optical micrographs of cracks and cavities found in the inner region of a new expansion joint.

characteristic, they are places prone to nucleation of cracks in presence of stresses of internal or external origin.

In Fig. 15 it is possible to note, in the straight section of the new metal expansion joint, the presence of pits and cracks that nucleate from such pits or discontinuities on the inner surface of the joint.

According to Fontana [4], localized corrosion, more precisely, pitting formation plays a key role in cracking. Pits or other discontinuities on the surface act as stress concentrators so that the stress in the pitting region may be greater than the material flow stress. Thus, if the component is subjected to tensile stresses of any nature (residual or applied), nucleation will occur and then its propagation, causing a possible component failure.

The tensile stress exerted on the material plays a fundamental role in the rupture of the passive layer of the stainless steels, so that the breaking of this passive layer accelerates the corrosion at several points of the surface, allowing the nucleation of cracks. The breakdown of the oxide layer added to the propagation of cracks, depending on the stresses that the component is subjected, do not allow the material to recover and the propagation becomes inevitable [4].

The presence of pits in the inner region of the new smooth tube suggests that pits probably formed at the storage or transport

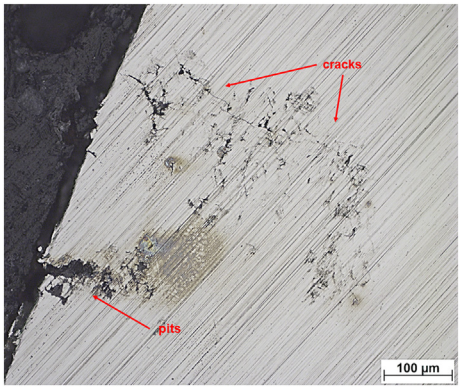

Fig. 15. Optical micrographs showing the straight section of a new metal expansion joint. Sample sanded in sandpaper with granulometry up to 1200 mesh.

stages of the tubes, considering that the internal region of the tube is an area of stagnation, where air circulation and moisture output is difficult.

3.4. X-ray diffraction

Fig. 16 shows the X-ray diffraction peaks obtained from the bellows samples of the metal expansion joint, the flat tube and the solution annealed smooth tube. The presence of deformation-induced martensite (BCC) is confirmed from the diffraction peaks of the flat tube and the bellows of the metal expansion joint. The solution annealed treatment performed on the smooth tube sample dissolves all the martensite, so that in this sample peaks refer only to the austenite diffraction planes.

3.5. Microhardness

Table 3 shows the microhardness values obtained in the inner and outer regions of the new metal expansion joint, the smooth pipe and solution annealed samples of the smooth pipe and the new metal expansion joint. It can be seen from Table 3 that the internal and external regions of the expansion joint flap have higher hardness values, in the range of 319–359 HV, to the values found in the smooth pipe that are in the range of 197 to 224 HV. The solution annealed parts of both the smooth tube and the expansion joint vent region showed the lowest hardness values (159–179 HV), which are lower than those recorded in the plain tube and the new metal expansion joint. The increase in hardness is related to the conformation process in which the component is subjected during its manufacture. The high values of microhardness found are an indication that the bellows exhibit a surface tension due to the cold forming process [20]. During the conformation process, the metastable austenite of the austenitic stainless steels, such as 304, leads to the formation of the martensite induced by deformation. This structure is associated with a volumetric expansion in relation to the austenitic matrix [21] and is accompanied by an increase in the density of dislocations, which results in an increase in local stress [22].

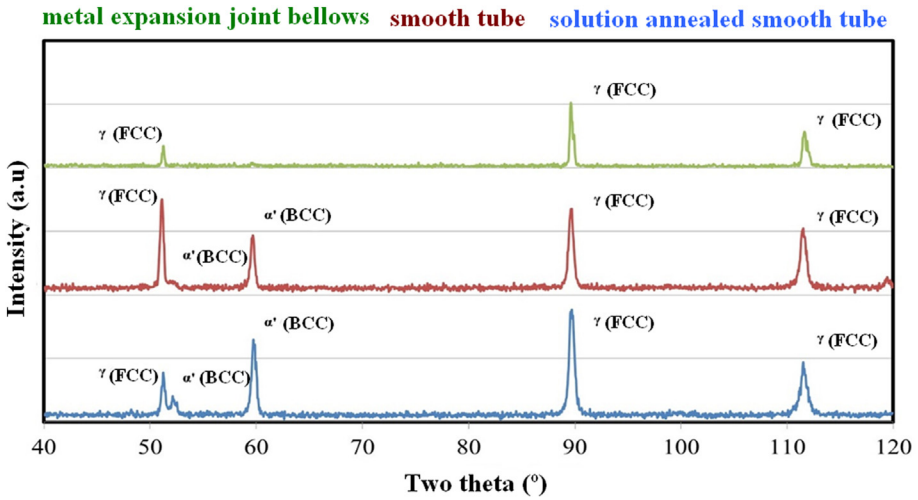

Fig. 16. X-ray diffraction peaks of the bellows samples of the metal expansion joint, the smooth tube and the solution annealed smooth tube.

Table 3.
Microhardness of the samples.

Samples	Average	Maximum	Minimum
A	345 ∓ 11 HV	359 HV	328 HV
B	337 ∓ 13 HV	357 HV	319 HV
L	213 ∓ 9 HV	224 HV	197 HV
L-SOL	171 ∓ 8 HV	179 HV	159 HV
B-SOL	170 ∓ 7 HV	179 HV	159 HV

Lozano-Peres et al., Scatigno et al. and Ryan et al. [11,23,24] state that for the occurrence of stress corrosion it is necessary that the material is subjected to at least three conditions: tensile (applied or residual), propitious environment and the material itself must have metallurgical conditions that favor corrosion. Fontana and Khatak et al. [4,9] indicate that austenitic stainless steels are susceptible to this type of corrosion, especially in environments containing chloride ions, since these ions are predominantly present in various media.

The martensitic structure observed in the new metal expansion bellows joints contribute to the embrittlement of the material and the consequence was the formation of cracks in addition to the reduction of their corrosion resistance. Deformation and the stress applied to the material during service induced martensite. AISI 304 is also susceptible to pitting corrosion which enhances the reduction of corrosion resistance.

4. Conclusions

The corrosion observed only inside of the bellows of the expansion joint and the stainless steel tube evidenced an inefficient cleaning of the region, which allowed the formation of cavities and pits in the place during the conditioning, transportation and installation of the components. The bellows manufacturing process, which consists of the conformation of a tube, allowed the formation of martensite induced by deformation as well as the accumulation of residual stress. The joint action of the residual tension, originated from the formation of the bellows during its manufacture; the tension applied during the service and the metallurgical conditions related to the martensitic structure favored the nucleation of cracks from the pits and pre-existing cavities that compromised the corrosion resistance of the component until its failure. As a recommendation, a set of standards can be adopted to avoid premature failure of these components. ASTM F1120-87 (2015) standard [25] lists a number of actions that can be taken regarding the cleaning and the transport of bellows of metal expansion bellows joints to avoid the premature formation of discontinuities that could compromise the use of the component. ASTM A269-15 standard [26] establishes a series of thermal treatments to be performed on stainless steel 300 series tubes to avoid the formation of undesirable phases in the steel as well as the accumulation of residual stress.

References

[1] P.K. Sen, H. Adeli, A new steel expansion joint for industrial plants: Bubble joint, Int. J. Press. Vessels Pip. 83 (2006) 447–463, https://doi.org/10.1016/j.ijpvp.2006.01.005.
[2] Witzenmann, Expantion Joint Manual, www.witzenmann.be/repo/assets/Expansion_joints_manual_1501uk_5_12_12_20.pdf, (2012) (accessed 7.11.2018).
[3] G. Wang, K.F. Zhang, D.Z. Wu, J.Z. Wang, Y.D. Yu, Superplastic forming of bellows expansion joints made of titanium alloys, J. Mater. Process. Technol. 178 (2006) 24–28, https://doi.org/10.1016/j.jmatprotec.2005.10.005.
[4] M.G. Fontana, Corrosion Engineering, 3rd ed, McGraw-Hill, New York, 1986.
[5] A.J. Sedriks, Corrosion of Stainless Steels, 2nd ed, John Wiley & Sons, New York, 1996.
[6] W.D. Callister, D.G. Rethwisch, Materials Science and Engineering, Vol. 5 John Wiley & Sons, New York, 2011.
[7] ASTM A262-15, Standard Practices for Detecting Susceptibility to Intergranular Attack in Austenitic Stainless Steels, ASTM International, West Conshohocken, PA, 2015http://www.astm.org/cgi-bin/resolver.cgi?A262-15 , Accessed date: 10 September 2018.
[8] T. Lyman, Metals Handbook: Atlas of Microstructures of Industrial Alloys, American Society for Metals, Ohio, 1972.
[9] H.S. Khatak, Corrosion of Austenitic Stainless Steels Mechanism, Mitigation and Monitoring, Woodhead, Cambridge, 2002.
[10] M. Milad, N. Zreiba, F. Elhalouani, C. Baradai, The effect of cold work on structure and properties of AISI 304 stainless steel, J. Mater. Process. Technol. 203 (2008) 80–85, https://doi.org/10.1016/j.jmatprotec.2007.09.080.
[11] S. Lozano-Perez, J. Dohr, M. Meisnar, K. Kruska, SCC in PWRs: learning from a bottom-up approach, Metall. Mater. Trans. E. 1 (2014) 194–210, https://doi.org/10.1007/s40553-014-0020-y.
[12] C.L. Briant, A.M. Ritter, The effects of deformation induced martensite on the sensitization of austenitic stainless steels, Metall. Trans. A. 11 (1980) 2009–2017, https://doi.org/10.1007/BF02655120.
[13] C.L. Briant, A.M. Ritter, The effect of cold work on the sensitization of 304 stainless steel, Scr. Metall. 13 (1979) 177–181, https://doi.org/10.1016/0036-9748(79)90288-6.
[14] A.F. Padilha, R.L. Plaut, P.R. Rios, Annealing of cold-worked austenitic stainless steels, ISIJ Int. 43 (2) (2003) 135–143.
[15] W.S. Lee, The morphologies and characteristics of impact-induced martensite in 304L stainless steel, Scr. Mater. 43 (2000) 777–782.
[16] K. Elayaperumal, P.K. De, J. Balachandra, Passivity of type 304 stainless steel–effect of plastic deformation, Corrosion 28 (1972) 269–273, https://doi.org/10.5006/0010-9312-28.7.269.
[17] U. Kamachi Mudali, N. Parvathavarthini, R. Dayal, J. Gnanamoorthy, Localized corrosion resistance of a new ferritic stainless steel, Trans. Indian Inst. Metals 41 (1988) 35–40.
[18] D. Kotecki, J. Lippold, Welding metallurgy and weldability of stainless steels, in: B. Barbero, E. Ureta (Eds.), 2011 Comp. Study Differ. Digit. Tech. Their Accuracy Comput Aided Des. 43 Wiley, Hoboken NJ, 2005, pp. 188–206.
[19] H. Colpaert, A.L.V. da Costa e Silva, Metallography of Common Steel Products, 4 Ed, Blucher, São Paulo, 2012.
[20] K.V. Kasiviswanathan, N.G. Muralidharan, N. Raghu, R.K. Dayal, H. Shaikh, Corrosion related failures of austenitic stainless steel components, Corros. Austenitic Stainl. Steels, Elsevier, 2002, pp. 314–339, , https://doi.org/10.1533/9780857094018.340.

[21] I. Mészáros, J. Prohászka, Magnetic investigation of the effect of α'-martensite on the properties of austenitic stainless steel, J. Mater. Process. Technol. 161 (2005) 162–168, https://doi.org/10.1016/j.jmatprotec.2004.07.020.
[22] S. Ghosh, V. Kain, Microstructural changes in AISI 304L stainless steel due to surface machining: effect on its susceptibility to chloride stress corrosion cracking, J. Nucl. Mater. 403 (2010) 62–67, https://doi.org/10.1016/j.jnucmat.2010.05.028.
[23] G.G. Scatigno, M.P. Ryan, F. Giuliani, M.R. Wenman, The effect of prior cold work on the chloride stress corrosion cracking of 304L austenitic stainless steel under atmospheric conditions, Mater. Sci. Eng. A 668 (2016) 20–29, https://doi.org/10.1016/j.msea.2016.05.037.
[24] M.P. Ryan, D.E. Williams, R.J. Chater, B.M. Hutton, D.S. McPhail, Why stainless steel corrodes, Nature 415 (2002) 770–774, https://doi.org/10.1038/415770a.
[25] ASTM F1120-87, Standard Specification for Circular Metallic Bellows Type Expansion Joints for Piping Applications, ASTM International, West Conshohocken, PA, 2015http://www.astm.org/cgi-bin/resolver.cgi?F1120-87 , Accessed date: 10 September 2018.
[26] ASTM A269/A269M-15a, Standard Specification for Seamless and Welded Austenitic Stainless Steel Tubing for General Service, ASTM International, West Conshohocken, PA, 2015http://www.astm.org/cgi-bin/resolver.cgi?A269A269M-15a , Accessed date: 10 September 2018.